

Article

Towards the Search for Thallium Nuclear Schiff Moment in Polyatomic Molecules: Molecular Properties of Thallium Monocyanide (TlCN)

A. V. Kudrin ¹, A. Zaitsevskii ^{1,2,*}, T. A. Isaev ², D. E. Maison ^{2,3} and L. V. Skripnikov ^{2,3}¹ Chemistry Department, M. Lomonosov Moscow State University, Moscow 119991, Russia² NRC “Kurchatov Institute”—PNPI, Orlova Roscha, 1, Gatchina 188300, Russia³ Physical Department, Saint-Petersburg State University, Ulianovskaya 1, Petrodvoretz 198504, Russia

* Correspondence: zaitsevskii_av@pnpi.nrcki.ru

Received: 29 April 2019; Accepted: 25 June 2019 ; Published: 29 June 2019



Abstract: Molecular properties of the thallium monocyanide (Tl·CN) system in its ground electronic state are studied using high-precision ab initio relativistic two-component pseudopotential replacing 60 inner-core electrons of Tl. A relativistic coupled-cluster method with single, double and perturbative triple amplitudes is employed to account for electronic correlations. Extrapolation of results to the complete basis set limit is used for all studied properties. The global potential energy minimum of Tl·CN corresponds to the linear cyanide (TlCN) isomer, while the non-rigid isocyanide-like (TlNC) structure lies by approximately 11 kJ/mol higher in energy. The procedure of restoration of the wavefunction in the “core” region of Tl atom was applied to calculate the interaction of the Tl nuclear Schiff moment with electrons. The parameter X of the interaction of the Tl nuclear Schiff moment with electrons in the linear TlCN molecule equals 7150 a.u. The prospects of using the TlCN molecule for the experimental detection of the nuclear Schiff moment are discussed.

Keywords: molecular electronic structure; parity and time-reversal invariance violating interactions; Schiff moment; relativistic coupled cluster calculation

PACS: 31.30.-j; 37.10.Mn; 12.15.Mm; 21.10.Ky

1. Introduction

Linear triatomic molecules with heavy atoms have recently attracted great attention in connection with the prospects for searching for the effects not described in the framework of the Standard Model of elementary particles. Some triatomic molecules with open-shell ground electronic states have been proposed for the search for the nuclear spin-dependent effects, violating space parity ($\mathcal{N}SD-\mathcal{P}\mathcal{V}$ effects) and scalar electron-nucleon interaction violating both space parity and time reversibility (\mathcal{P}, \mathcal{T} -odd effects) [1,2] and search for permanent electron electric dipole moment [3]. It turns out that linear triatomic molecules with Σ ground electronic state (like the proposed RaOH and YbOH), being excited to the first bending vibrational state, possess so-called l -doubling of spin-rotational levels, similar to Λ -doubling for spin-rotational levels for linear molecules with Π ground electronic state. The Λ -doubling can be, for example, used with great efficiency for suppressing of the different systematic effects in ultra-precise molecular spectroscopy (see e.g., Reference [4]). Recently, the search for the Schiff moment of the Tl nucleus has started using the TlF molecule [5] and the spin-rotational spectrum of this molecule was studied for both ground and several excited states [6]. In Reference [1] we have pointed to the molecule TlCN as a prospective candidate for the search for $\mathcal{N}SD-\mathcal{P}\mathcal{V}$ and \mathcal{P}, \mathcal{T} -odd effects (note that the nuclear Schiff moment arises due to \mathcal{P}, \mathcal{T} -odd nuclear forces). Both experimental and theoretical information concerning the molecular structure and isomerism of TlCN is scarce. Three

vibrational frequencies detected in the gas-phase experiment [7] were allegedly assigned to cyanide and isocyanide isomers. The DFT electronic structure calculations [7] using large-(68-electron-) core one-component pseudopotential of Tl and a very restricted basis set, confirmed the existence of linear TICN, whereas the detected stationary point of the potential energy surface presumably associated with the isocyanide was a saddle-type point.

According to electronic structure calculations and experiments in the gas phase and in inert matrices, molecules consisting of a group 13 or group 1 metal atom M and the CN fragment, M·CN, which can be considered respectively as analogs and pseudo analogs of Tl·CN, can have linear or slightly bent isomers (the cyanide MCN and isocyanide MNC) and a T-shaped one usually denoted as M[CN]. In the first approximation, the relative stability of isomers is determined by the type of the M–CN bond. If this bond is essentially ionic, the T-shaped structure is normally the most stable one due to the optimal Coulomb attraction and the isomerization barriers are low [8]. This situation occurs in the Na·CN [9–11] and K·CN [10–13] molecules. In the latter case, the KNC isomer does not exist [11]. In contrast, when the bond has a significant covalent component, isocyanide structures are more stable, isomerization barriers are relatively large and the T-shaped isomers usually do not exist [14]. It seems natural to suppose the existence of linear TICN isomers similar to those of other cyanides of 13th groups elements.

In the present paper we report a study of ground-state properties and isomerism of Tl·CN by accurate relativistic electronic structure methods and for the first time calculate the parameter X of the interaction of the Tl nuclear Schiff moment [15] with electrons in linear triatomic molecule, TICN.

2. Computational Methods

The electron subsystem of Tl·CN is described using the accurate shape-consistent two-component relativistic pseudopotential replacing 60 inner-core ($1s$ – $4f$) electrons of the Tl atom [16]. The remaining external electrons of Tl and all the electrons of the light atoms are treated explicitly. The many-electron problem is solved using the relativistic coupled-cluster method with single, double and perturbative triple cluster amplitudes, RCCSD(T) [17] with the triple zeta (TZ) and quadruple zeta (QZ) quality basis sets. The TZ set includes aug-cc-pVTZ bases for C, N [18] and $(9s\ 9p\ 8d\ 4f\ 1g) / [6s\ 7p\ 5d\ 4f\ 1g]$ one for Tl [19]; the QZ set consists of aug-cc-pVQZ for C, N [18] and $(10s\ 11p\ 9d\ 5f\ 4g\ 1h) / [7s\ 8p\ 6d\ 5f\ 4g\ 1h]$ for Tl [19]. One-electron molecular spinors are constructed by solving the relativistic Kramers-restricted analog of the Hartree–Fock equations. Final energy estimates are obtained by the two-point extrapolation to the complete basis set limit (CBS) [20]. Note that the extrapolation efficiently suppresses the basis set superposition errors [21]. A separate set of calculations is performed using the two-component relativistic density functional theory (RDFT) [22] with the hybrid exchange–correlation functional PBE0 [23] and the basis sets $(11s\ 7p\ 2d) / [5s\ 4p\ 2d]$ for C, N [24] and uncontracted $[8s\ 7p\ 7d\ 3f]$ for Tl [16].

We started with scanning the RCCSD(T) potential energy surface in a wide range of the internal coordinates R and θ (see Figure 1) in order to approximately locate the stationary points. At this stage, the C–N distance was frozen at $r(\text{CN}) = 1.158\ \text{\AA}$. Then the configurations and energies of all linear structure were refined using the Broyden–Fletcher–Goldfarb–Shanno’s algorithm [25].

The vibrational frequencies for the TICN isomer (Tl–C stretching ω_1 , bending ω_2 and $\text{C}\equiv\text{N}$ stretching ω_3) are evaluated within the harmonic approximation. Other molecular properties of this isomer are calculated for the equilibrium geometry obtained at the CBS limit. The dipole moment D is evaluated within the central finite-difference approximation, fitting the dependence of the total energy on the strength of the applied uniform electric field along the molecular axis in the range $\pm 0.00004\ \text{a.u.}$

The effective interaction of electrons with the Tl nuclear Schiff moment in the TICN molecule is described by the following Hamiltonian [15,26]:

$$H_{\text{eff}} = 6X \left(\vec{S}, \vec{\lambda} \right), \quad (1)$$

where $\vec{S}=\vec{S}I/I$ is the Schiff moment of TI, \vec{I} is TI nuclear spin, $\vec{\lambda}$ is the unit vector along the internuclear axis z from TI to C and X is the parameter given by:

$$X = \frac{2\pi}{3} \cdot \left. \frac{\partial \rho_{\psi}(\vec{r})}{\partial z} \right|_{\vec{r}=0}, \quad (2)$$

where $\rho_{\psi}(\vec{r})$ is the electronic density at the point \vec{r} , where $\vec{r} = 0$ corresponds to the center of the TI nucleus. To calculate this parameter determined by the behavior of the valence wave function inside the nucleus, we employed the two-step method described in detail in References [27–31]. At the first step, the valence and outer-core part of the molecular wave function is treated within the generalized relativistic pseudopotential method [32–34]. The inner-core electrons are excluded from the explicit treatment. The resulting valence (pseudo) wave functions are smoothed in the spatial inner core region of a heavy atom that leads to considerable computational savings [35,36]. The second step is the nonvariational restoration of the correct 4-component behavior of the valence wave function in the spatial core region of the heavy atom [27–31].

The calculations are carried out using the DIRAC17 [37], MRCC [38,39], and two-component relativistic DFT [22] codes.

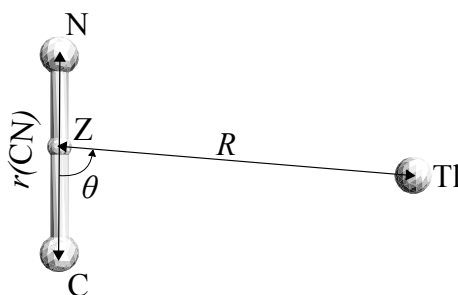


Figure 1. Internal coordinates R , $r(\text{CN})$, θ for the Thallium Monocyanide (TI-CN) system. Z is the center of mass of the CN fragment, $\theta = 0^\circ$ and $\theta = 180^\circ$ correspond to the linear TICN and TINC structures, respectively.

3. Results and Discussion

Molecular properties. The relative energies of stationary points for the TI-CN potential energy surface are listed and compared with the corresponding values for the cyanides of group 13 and 1 elements in Table 1. At all levels of correlation treatment (RCCSD(T)/TZ,QQ,CBS, RDFT/PBE0) the global energy minimum corresponds to the linear TICN isomer. The dependence of the ground-state energy on the bending angle in the region of isocyanide-like structures is extremely flat. The cross section of TI-CN potential energy surface along the approximate isomerization path obtained at the RCCSD(T)/CBS level of theory is displayed in Figure 2.

Due to the non-rigidity of the TINC-like structure, the position of the local minimum is very sensitive to the level of correlation treatment; the harmonic approximation for the vibrations of this isomer is senseless.

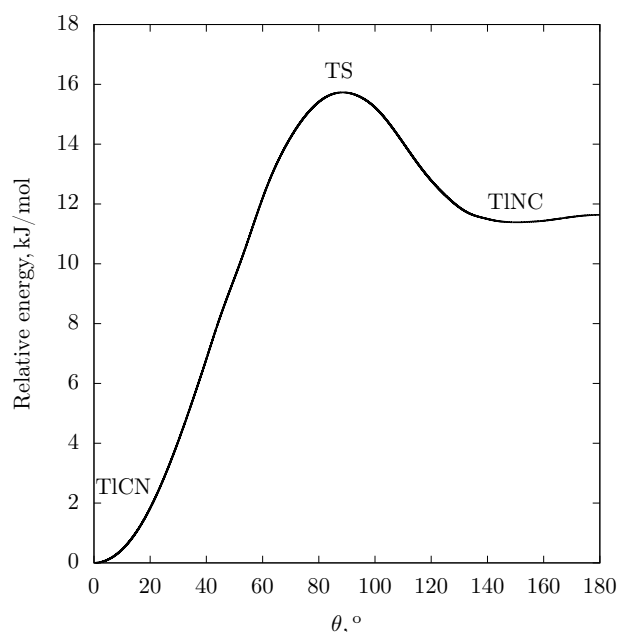


Figure 2. The cross section of RCCSD(T)/CBS potential energy surface for TI·CN along the approximate isomerization path. TS: transition state. The energy is given with respect to the global minimum. The distance $r(\text{CN}) = 1.16641 \text{ \AA}$ is frozen at the equilibrium value for the TICN isomer.

Table 1. Relative energies (kJ/mol) of isomers and transition states (TS) for M·CN systems. PW: present work.

M	Method	Source	MCN	TS	MNC		
					Minimum	Linear	
Tl	RCCSD(T)/TZ	PW	0	16.4		9.0	
	RCCSD(T)/QZ		0	16.0	9.9	11.2	
	RCCSD(T)/CBS		0	15.7	10.7	11.4	
Tl	RDFT/PBE0		0		13.4	14.5	
	DFT/BP89	[7]	0			6.2	
Al	CCSD	[40]	25.7	55.5		0	
	CCSD(T)	[40]	23.2			0	
	QCISD(T)	[41]	23.7			0	
Ga	DFT/BP89	[7]	5.5			0	
	DFT/B3LYP	[42]	8.7			0	
In	DFT/BP89	[7]	1.4			0	
			MCN	TS	M[CN]	linear MNC	
Na	CCSD(T)	[11]	10.1	15.8	0	11.2	
K	CCSD(T)	[11]	18.3	19.3	0	13.0	—
Rb	CCSD(T)	[11]	18.3	18.8	0	12.5	

The situation with no minima corresponding to the linear isocyanide structure and low isomerization barriers is typical for systems with predominantly ionic bonds M·CN. At the same time, for strongly ionic alkali metal cyanides the most stable isomers are T-shaped. In contrast, light analogues of the thallium compounds, such as the Al·CN and Ga·CN, are stable in the isocyanide configurations and have no T-shaped isomers. Along the series Al–Ga–In–Tl, the relative stability of the isocyanide isomers decreases monotonically, so that the TICN isomer is significantly more stable than the isocyanide. The isomerisation barriers decrease along the series, becoming for the Tl·CN comparable to those in Na·CN, K·CN and Rb·CN systems. The results of simple DFT modeling of the indium system (Table 1) indicate that the linear InNC should not exist; however, this disagrees with the microwave spectroscopy data [42]. Anyway, according to the infrared spectroscopy study [7] the linear or slightly bent InNC is slightly more abundant than the cyanide.

The calculated equilibrium geometries, harmonic vibrational frequencies and dipole moment for the TICN isomer, along with the corresponding available experimental data for other analogue and pseudo analogue M·CN systems, are collected in Table 2. The TICN harmonic vibrational frequencies were calculated for the most abundant isotopomer ($^{205}\text{Tl}^{12}\text{C}^{14}\text{N}$). In all cases, the dipole moment direction corresponds to the charge redistribution $\text{M}^{+\delta}\cdot(\text{CN})^{-\delta}$.

Table 2. Molecular parameters of M·CN isomers for M belonging to groups 13 and 1. Internuclear distances in ångstroms, vibrational frequencies (ω) in cm^{-1} , dipole moments (D) in atomic units, $r(\text{MX}) = r(\text{MC})$ for cyanides and $r(\text{MN})$ for isocyanides. PW: present work.

Molecule	Source	$r(\text{MX})$	$r(\text{CN})$	ω_1	ω_2	ω_3	D	
TICN	RCCSD(T)/TZ, PW	2.344	1.173					
	RCCSD(T)/QZ, PW	2.333	1.170					
	RCCSD(T)/CBS, PW	2.324	1.166	294	101	2163	2.41	
	RDFT/PBE0, PW	2.358	1.178	277	104	2149	2.39	
TICN	Exptl. [7]					2126		
TINC(?)	Exptl. [7]			307(?)		2048		
AICN	CCSD(T) [40]	2.014	1.171	472	187	2479	3.49	
	Exptl. [41]			524	133	1975		
	Exptl. [7]			456		2144		
AINC	CCSD(T) [40]	1.861	1.187	584	131	2290	3.14	
	Exptl. [42]	1.854	1.178	453	167			
	Exptl. [43]	1.849	1.171					
GaCN	Exptl. [44]			549;557	100	2069		
	Exptl. [7]			532		2069		
	Exptl. [42]	2.062	1.158	304				
GaNC	Exptl. [7]					2138		
	Exptl. [42]	1.938	1.174		105			
InCN	Exptl. [7]			401		2046		
	Exptl. [42]	2.262	1.146	302				
InNC	Exptl. [7]			333		2132		
	Exptl. [42]	2.137	1.170		71			
	Exptl. [7]			392		2151		
		$r(\text{MC})$	$r(\text{MN})$	$r(\text{CN})$	ω_1	ω_2	ω_3	D
Na[CN]	Exptl. [9]	2.366	2.243	1.169				
	Exptl. [45]				368	168	2047	
	CCSD(T) [11]	2.39	2.23	1.18				3.48
K[CN]	Exptl. [12]	2.716	2.549	1.169				
	Exptl. [45]				288	139	2050	
	CCSD(T) [11]	2.73	2.55	1.18				4.04

Unusually flat bending potentials and large amplitudes of zero-point vibrations in Al, Ga and In isocyanides were discussed in Reference [42]. The shape of the bending potential of the TINC isomer (Figure 2) apparently indicates that the bending motion is fairly free in the range $\theta = 140^\circ \dots 220^\circ$. Note that the computed TICN bending frequency $\omega_2 = 101.2 \text{ cm}^{-1}$ also corresponds to the significant zero-point vibration amplitude.

The calculated TICN equilibrium geometry corresponds to the rotational constant value $B_e = 2.406 \text{ GHz}$. The l doubling interval can be roughly estimated as $B^2/\omega_2 = 1.9 \text{ MHz}$. This value is significantly smaller than its counterparts for the systems recently proposed for the search for $\mathcal{N}SD\text{-}\mathcal{P}\mathcal{V}$ and \mathcal{P}, \mathcal{T} -odd effects, RaOH (3.1 MHz) [1] and YbOH, where the value of l -doubling splitting was estimated to be $\approx 10 \text{ MHz}$ [3]. The TICN l -doubling interval is expected to be the smallest one for group 13 (iso)cyanide molecules; even for the rather heavy and flexible InNC molecule, the l -doubling interval should be about 4.6 MHz. Thus full polarisation of the TICN molecule can be reached in electric fields smaller than 100 V/cm , which allows much better control of the systematic effects in high-precision experiments.

For all group 13 and group 1 atoms, the $\text{C}\equiv\text{N}$ stretching frequencies in M·CN are in the ranges ca. $2125\text{--}2150 \text{ cm}^{-1}$ for cyanide isomers and ca. $2040\text{--}2050 \text{ cm}^{-1}$ for isocyanide or T-shaped isomers. The only unexpected experimental value for the AICN molecule obtained by Fukushima [41] ($\omega_3 = 1974.5 \text{ cm}^{-1}$) disagrees with another experimental estimate ($\omega_3 = 2143.7 \text{ cm}^{-1}$ [7]) and the

results of electronic structure calculations. Our estimate $\omega_3 = 2163 \text{ cm}^{-1}$ for TICN is in line with this pattern.

The RCCSD(T) dipole moment values for TICN seem unexpectedly small even compared to that of AICN and AINC molecules where the covalent contribution to Al-CN bonding is believed significant.

Schiff moment. The values of the X parameter for the TICN molecule obtained within different basis sets and methods are given in Table 3. One can see a good convergence of the results with increasing basis set size. In particular, the contribution of the perturbative triple cluster amplitudes is almost independent of basis set size, being smaller than 3%. This also demonstrates a good convergence with respect to the level of the electron correlation treatment.

Table 3. Calculated values of the X parameter for TICN. The recommended estimate is given in boldface.

Basis Set		X , a.u.		
Tl	C, N	Hartree-Fock	RCCSD	RCCSD(T)
[6s7p5d4f1g]	[5s4p3d2f]	8997	7119	6939
[9s9p8d4f1g]	[5s4p3d2f]	9093	7263	7076
[7s8p7d5f4g1h]	[6s5p4d3f]	9105	7351	7150

The final X value (7150 a.u.) is close to that obtained earlier for the ^{205}TlF molecule (7635 a.u., [27]).

If the properties of the excited electronic states in TICN resemble those in TlF, one would also expect amenability of TICN for cooling with lasers. This would open an exciting perspective for the ultra-precision spectroscopy of polyatomic molecules with closed electronic shells. The resulting value of the X parameter is also close to that for the ^{225}RaO (7532 a.u. [46]) and ^{207}PbO [30] molecules and about two times larger than in the ^{225}RaF molecule [47]. Just to compare the Schiff moment enhancement factor with non-molecular systems, we notice that the X parameter, for example, liquid xenon is almost 40 times smaller [48].

4. Conclusions

The results of relativistic calculations on the ground electronic state of the Tl-CN system in the framework of the coupled cluster (RCCSD(T)) method with the extrapolation to the complete basis set limit demonstrate unambiguously that the lowest-energy isomer has a linear cyanide-like (TICN) equilibrium structure. The isocyanide-like isomer has equilibrium energy 11 kJ/mol above the global minimum and is extremely non-rigid with respect to bending deformations. Similar results were obtained within the simple relativistic density functional computational scheme. In the Al-Tl row of cyanides and isocyanides the Tl-CN system is probably the first wherein the cyanide TICN is the most stable isomer. Along this row, the rigidity of cyanides and isocyanides gradually decreases. Our estimate of the parameter characterising the interaction of the Tl nuclear Schiff moment with electrons in the TICN isomer is close to that obtained earlier for TlF [27] and the analogous parameter for the Ra nucleus in RaO [46]. We conclude that the TICN molecule has good prospects for searching for effects outside of the Standard Model.

Author Contributions: Conceptualization, A.Z. and T.A.I.; Data curation, A.V.K. and D.E.M.; Formal analysis, A.V.K. and D.E.M.; Methodology, A.Z. and L.V.S.; Supervision, A.Z. and T.A.I.

Funding: This research was funded by RSF grant number 18-12-00227.

Acknowledgments: We are indebted to C. van Wüllen for providing us with his relativistic DFT code [22]. Schiff moment calculation including basis set generation are supported by RSF Grant No. 18-12-00227. T.A.I. thanks participants of the NPCCM2018 workshop (MITP, Mainz, 26-30 November 2018) for inspiring discussions.

Conflicts of Interest: The authors declare no conflict of interest. The funders had no role in the design of the study; in the collection, analyses, or interpretation of data; in the writing of the manuscript, or in the decision to publish the results.

References

1. Isaev, T.A.; Zaitsevskii, A.V.; Eliav, E. Laser-coolable polyatomic molecules with heavy nuclei. *J. Phys. B At. Mol. Opt. Phys.* **2017**, *50*, 225101. [CrossRef]
2. Norrgard, E.B.; Barker, D.S.; Eckel, S.P.; Fedchak, J.A.; Klimov, N.N.; Scherschligt, J. Nuclear-Spin Dependent Parity Violation in Optically Trapped Polyatomic Molecules. *arXiv* **2018**, arXiv:1812.00064.
3. Kozyryev, I.; Hutzler, N. Precision measurement of time-reversal symmetry violation with laser-cooled polyatomic molecules. *Phys. Rev. Lett.* **2017**, *119*, 133002. [CrossRef] [PubMed]
4. Shafer-Ray, N.E. Possibility of 0-g- factor paramagnetic molecules for measurement of the electron's electric dipole moment. *Phys. Rev. A* **2006**, *73*, 034102. [CrossRef]
5. DeMille, D. CeNTREX Experiment (DAMOP 2017 Report). (2017). Available online: <http://meetings.aps.org/Meeting/DAMOP17/Session/B2.3> (accessed on 29 April 2019).
6. Norrgard, E.B.; Edwards, E.R.; McCarron, D.J.; Steinecker, M.H.; DeMille, D.; Alam, S.S.; Peck, S.K.; Wadia, N.S.; Hunter, L.R. Hyperfine structure of the $B^3\Pi_1$ state and predictions of optical cycling behavior in the $x \rightarrow B$ transition of TlF. *Phys. Rev. A* **2017**, *95*, 062506. [CrossRef]
7. Lanzisera, D.V.; Andrews, L. Reactions of Laser-Ablated Al, Ga, In, and Tl Atoms with Hydrogen Cyanide in Excess Argon. Matrix Infrared Spectra and Density Functional Theory Calculations on New Cyanide and Isocyanide Products. *J. Phys. Chem. A* **1997**, *101*, 9660. [CrossRef]
8. Essers, R.; Tennyson, J.; Wormer, P. An SCF potential energy surface for Lithium Cyanide. *Chem. Phys. Lett.* **1982**, *89*, 223. [CrossRef]
9. Van Vaals, J.; Meerts, W.L.; Dymanus, A. Structure of sodium cyanide by molecular beam electric resonance spectroscopy. *J. Chem. Phys.* **1982**, *77*, 5245. [CrossRef]
10. Marsden, C. Ab initio correlated potential energy surfaces for monomeric sodium and potassium cyanides. *J. Chem. Phys.* **1982**, *76*, 6451. [CrossRef]
11. Lee, D.-K.; Lim, I.S.; Lee, Y.S.; Hagebaum-Reignier, D.; Jeung, G.-H. Molecular properties and potential energy surfaces of the cyanides of the groups 1 and 11 metal atoms. *J. Chem. Phys.* **2007**, *126*, 244313. [CrossRef]
12. Van Vaals, J.; Meerts, W.L.; Dymanus, A. Molecular beam electric resonance study of KCN, K13CN and KC15N. *J. Mol. Spectrosc.* **1984**, *106*, 280. [CrossRef]
13. Törring, T.; Bekooy, J.; Meerts, W.L.; Hoeft, J.; Tiemann, E.; Dymanus, A. Rotational spectrum and structure of KCN. *J. Chem. Phys.* **1980**, *73*, 4875. [CrossRef]
14. Petrie, S. Trends in M (CN) isomerism: A computational study of monocyanides of the main-group third row atoms. *Phys. Chem. Chem. Phys.* **1999**, *1*, 2897. [CrossRef]
15. Hinds, E.A.; Sandars, P.G.H. Electric dipole hyperfine structure of TlF. *Phys. Rev. A* **1980**, *21*, 471. [CrossRef]
16. Available online: <http://www.qchem.pnpi.spb.ru> (accessed on 29 April 2019).
17. Vissler, L.; Lee, T.J.; Dyall, K.G. Formulation and implementation of a relativistic unrestricted coupled-cluster method including noniterative connected triples. *J. Chem. Phys.* **1996**, *105*, 8769. [CrossRef]
18. Dunning, T. H., Jr. Gaussian basis sets for use in correlated molecular calculations. I. The atoms boron through neon and hydrogen. *J. Chem. Phys.* **1989**, *90*, 1007. [CrossRef]
19. Zaitsevskii, A.; Eliav, E. Padé extrapolated effective Hamiltonians in the Fock space relativistic coupled cluster method. *Int. J. Quantum Chem.* **2018**, *118*, e25772. [CrossRef]
20. Petersson, G. A.; Frisch, M. J. A journey from generalized valence bond theory to the full CI complete basis set limit. *J. Phys. Chem. A* **2000**, *104*, 2183. [CrossRef]
21. Mourik, V.T.; Wilson, A.K.; Peterson, K.A.; Woon, D.E.; Dunning, J.T.H. *Advances in Quantum Chemistry*; Elsevier: Amsterdam, The Netherlands, 1998; Volume 31, pp. 105–135.
22. van Wüllen, C. A quasirelativistic two-component density functional and hartree-fock program. *Zeitschrift für Physikalische Chemie* **2010**, *224*, 413–426. [CrossRef]
23. Adamo, C.; Barone, V. Toward reliable density functional methods without adjustable parameters: The PBE0 model. *J. Chem. Phys.* **1999**, *110*, 6158. [CrossRef]
24. Godbout, N.; Salahub, D.R.; Andzelm, J.; Wimmer, E. Optimization of Gaussian-type basis sets for local spin density functional calculations. Part I. Boron through neon, optimization technique and validation. *Can. J. Chem.* **1992**, *70*, 560. [CrossRef]
25. Byrd, R.H.; Lu, P.; Nocedal, J.; Zhu, C. A limited memory algorithm for bound constrained optimization. *SIAM J. Sci. Comput.* **1995**, *16*, 1190. [CrossRef]

26. Sushkov, O.P.; Flambaum, V.V.; Khriplovich, I. B. Possibility of investigating P-and T-odd nuclear forces in atomic and molecular experiments. *Sov. Phys. JETP* **1984**, *87*, 1521.
27. Petrov, A.N.; Mosyagin, N.S.; Isaev, T.A.; Titov, A.V.; Ezhov, V.F.; Eliav, E.; Kaldor, U. Calculation of *P, T*-Odd Effects in ^{205}TlF Including Electron Correlation. *Phys. Rev. Lett.* **2002**, *88*, 073001. [[CrossRef](#)] [[PubMed](#)]
28. Titov, A.V.; Mosyagin, N.S.; Petrov, A.N.; Isaev, T.A.; DeMille, D.P. P, T-parity violation effects in polar heavy-atom molecules. *Prog. Theor. Chem. Phys.* **2006**, *15*, 253.
29. Skripnikov, L.V.; Titov, A.V. Theoretical study of ThF^+ in the search for T,P-violation effects: Effective state of a Th atom in ThF^+ and ThO compounds. *Phys. Rev. A* **2015**, *91*, 042504. [[CrossRef](#)]
30. Skripnikov, L.V.; Titov, A.V. LCAO-based theoretical study of PbTiO_3 crystal to search for parity and time reversal violating interaction in solids. *J. Chem. Phys.* **2016**, *145*, 054115. [[CrossRef](#)] [[PubMed](#)]
31. Skripnikov, L.V.; Titov, A.V.; Petrov, A.N.; Mosyagin, N.S.; Sushkov, O.P. Enhancement of the electron electric dipole moment in Eu^{2+} . *Phys. Rev. A* **2011**, *84*, 022505. [[CrossRef](#)]
32. Titov, A.V.; Mosyagin, N.S. Generalized relativistic effective core potential: Theoretical grounds. *Int. J. Quantum Chem.* **1999**, *71*, 359. [[CrossRef](#)]
33. Mosyagin, N.S.; Zaitsevskii, A.V.; Titov, A.V. Shape-consistent relativistic effective potentials of small atomic cores. *Rev. At. Mol. Phys.* **2010**, *1*, 63.
34. Mosyagin, N.S.; Zaitsevskii, A.V.; Skripnikov, L.V.; Titov, A.V. Generalized relativistic effective core potentials for actinides. *Int. J. Quantum Chem.* **2016**, *116*, 301. [[CrossRef](#)]
35. Skripnikov, L.V. Combined 4-component and relativistic pseudopotential study of ThO for the electron electric dipole moment search. *J. Chem. Phys.* **2016**, *145*, 214301. [[CrossRef](#)] [[PubMed](#)]
36. Skripnikov, L.V.; Mosyagin, N.S.; Titov, A.V. Relativistic coupled-cluster calculations of spectroscopic and chemical properties for element 120. *Chem. Phys. Lett.* **2013**, *555*, 79. [[CrossRef](#)]
37. Visscher, L.; Jensen, H.J.A.; Bast, R.; Saue, T.; Bakken, V.; Dyall, K.G.; Dubillard, S.; Ekström, U.; Eliav, E.; Enevoldsen, T.; et al. DIRAC, a Relativistic Ab Initio Electronic Structure Program, Release DIRAC17 (2017). Available online: <http://www.diracprogram.org> (accessed on 29 April 2019).
38. Kállay, M.; Rolik, Z.; Ladjángszki, I.; Szegedy, L.; Ladóczki, B.; Csontos, J.; Kornis, B. MRCC, a quantum chemical program suite. Available online: www.mrcc.hu (accessed on 29 April 2019).
39. Rolik, Z.; Kállay, M. A general-order local coupled-cluster method based on the cluster-in-molecule approach. *J. Chem. Phys.* **2011**, *135*, 104111. [[CrossRef](#)]
40. Ma, B.; Yamaguchi, Y.; Schaefer, H.F., III. Spectroscopic constants and potential energy surfaces for the possible interstellar molecules A1NC and A1CN. *Mol. Phys.* **1995**, *86*, 1331. [[CrossRef](#)]
41. Fukushima, M. Laser induced fluorescence spectroscopy of A1NC/A1CN in supersonic free expansions. *Chem. Phys. Lett.* **1998**, *283*, 337. [[CrossRef](#)]
42. Walker, K.A.; Evans, C.J.; S.-Suh, H.K.; Gerry, M.C.; Watson, J.K. Fourier Transform Microwave Spectroscopy of Cyanides and Isocyanides of Al, Ga, and In. *J. Mol. Spectrosc.* **2001**, *209*, 178. [[CrossRef](#)]
43. Robinson, J.; Apponi, A.; Ziurys, L. The millimeter-wave spectrum of A1NC: chemical trends in metal isocyanide molecules. *Chem. Phys. Lett.* **1997**, *278*, 1. [[CrossRef](#)]
44. Gerasimov, I.; Yang, X.; Dagdigian, P.J. Laser fluorescence excitation spectra of the A1NC and A1CN isomers. *J. Chem. Phys.* **1999**, *110*, 220. [[CrossRef](#)]
45. Ismail, Z.K.; Hauge, R.H.; Margrave, J.L. Infrared spectra of matrix-isolated sodium and potassium cyanides. *J. Mol. Spectrosc.* **1973**, *45*, 304. [[CrossRef](#)]
46. Kudashov, A.D.; Petrov, A.N.; Skripnikov, L.V.; Mosyagin, N.S.; Titov, A.V.; Flambaum, V.V. Calculation of the parity- and time-reversal-violating interaction in ^{225}RaO . *Phys. Rev. A* **2013**, *87*, 020102(R). [[CrossRef](#)]
47. Kudashov, A.D.; Petrov, A.N.; Skripnikov, L.V.; Mosyagin, N.S.; Isaev, T.A.; Berger, R.; Titov, A.V. Ab initio study of radium monofluoride (RaF) as a candidate to search for parity- and time-and-parity-violation effects. *Phys. Rev. A* **2014**, *90*, 052513. [[CrossRef](#)]
48. Isaev, T.A.; Petrov, A.N.; Mosyagin, N.S.; Titov, A.V. Search for the nuclear Schiff moment in liquid xenon. *Phys. Rev. A* **2007**, *75*, 032515. [[CrossRef](#)]

